Fe(III) oxo-complex containing salinomycinate and hydroxo ligands

N. N. Petkov [1], I. N. Pantcheva [1]*, R. R. Kukeva [2], D. G. Paneva [3], Z. P. Cherkezova-Zheleva [3], P. D. Dorkov [4]

[1] *Department of Analytical Chemistry, Faculty of Chemistry and Pharmacy, Sofia University "St. Kl. Ohridski", 1, James Bourchier Blvd., 1164 Sofia, Bulgaria*
[2] *Institute of General and Inorganic Chemistry, Bulgarian Academy of Sciences, Acad. Georgi Bonchev Str., Bldg. 11, 1113 Sofia, Bulgaria*
[3] *Institute of Catalysis, Bulgarian Academy of Sciences, Acad. Georgi Bonchev Str., Bldg. 11, 1113 Sofia, Bulgaria*
[4] *Research and Development Department, Biovet Ltd., 39, Peter Rakov Str., 4550 Peshtera, Bulgaria*

In this study we present the properties of a trinuclear ferric oxo-complex derived from the reaction of ionophorous antibiotic salinomycinic acid with Fe(II) ions. It was characterized by IR, EPR and Mössbauer spectroscopies, and thermogravimetric analysis. The data reveal the oxidation of Fe(II) to Fe(III) during the isolation of the final product and the involvement of salinomycin as a monoanion bridging metal ions. The effect of Fe(III) ions on the antibacterial efficacy of the parent ligand was assessed towards a panel of three Gram-positive microorganisms: *Bacillus subtilis*, *Bacillus cereus* and *Kocuria rhizophila*.

Keywords: polyether ionophore, triangular Fe(III) complex, antibacterial activity

INTRODUCTION

At the present, the research in cancer treatment has shown the undoubted potential of polyether ionophores as promising anticancer agents [1−9]. Among them is salinomycinic acid (SalH, Fig. 1) applied in the therapy of severe infectious diseases due to its coccidiostatic and antibacterial properties [10−15]. In addition, salinomycin possesses well documented *in vitro* anticancer efficacy [16−19], and although very rare, the case studies with volunteers show considerable success. These findings disclose the possibility for "old drugs" to be repurposed for new applications in the fight against cancer alongside the already proven in practice taxanes, vinca alkaloids, mytomycins, camptothecin and podophyllotixin derivatives.
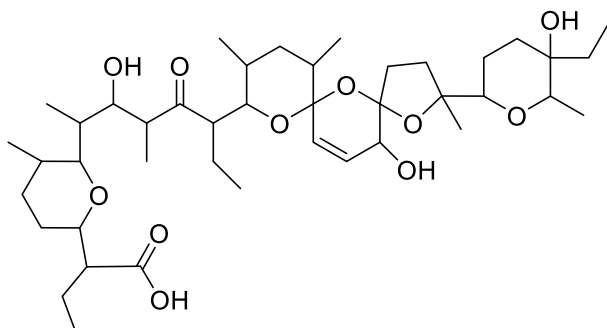

Fig. 1. Chemical structure of SalH

The high selectivity of salinomycin against cells with mitotic cycle disorder of benign or malignant origin [20] allows its administration at lower doses reducing the adverse drug effects. Moreover, the antibiotic exhibits significant bias towards cancer stem cells which are responsible for metastasis formation. The propensity of any chemotherapy candidate to inhibit the tumor development at stem cells level is a rare property and deserves comprehensive characterization at various perspectives. For that reason, we have initiated a thorough research on the chemical properties of salinomycin, including its interactions with various macro- and microelements [21−25].

One of the metal ions with a proven biological role in the cell life cycle is iron. It participates in the chain scavenging processes of oxidative phosphorylation but is also involved in generating radicals by Fenton's reaction to cause cell death *via* ptosis [26−33]. Among the possible ways of inducing changes in iron metabolism is the alteration of its concentration using Fe(II)/Fe(III) complexes with different ligands.

Recently we studied the complex-formation ability of salinomycin and monensin (the widest used polyether ionophore) to find that they can bind iron(III) ions as di- or trinuclear coordination species [25, 34]. The reaction conditions appear to be the crucial factor which determines the structure of the resulting products. In attempts to capture ferrous ions, we explored the coordination behavior of

* To whom all correspondence should be sent:
E-mail: *ahip@chem.uni-sofia.bg*

salinomycin in the presence of $FeSO_4$ as a starting metal salt. The paper describes the properties of the obtained salinomycinate, which indicate the metal ion oxidation and the formation of a triangular oxo-complex containing hydroxo ligands as well.

EXPERIMENTAL

Materials

Sodium salinomycinate (SalNa, p. a.) was supplied by Biovet Ltd. (Peshtera, Bulgaria). Salinomycinic acid (SalH) was prepared according to the procedure given by Gertenbach and Popov [35]. Fe(II) sulfate heptahydrate, Et_3N, MeOH, nutrient agar and sterile plastic ware were delivered by local suppliers. The aerobic bacterial strains *B. subtilis* (NBIMCC 1709), *B. cereus* (NBIMCC 1085) and *K. rhizophila* (NBIMCC 159) were supplied by the National Bank for Industrial Microorganisms and Cell Cultures (NBIMCC, Bulgaria).

Synthesis of complex 1

To a solution containing SalH (1.0 mmol, 751.0 mg in 20 mL MeOH) and Et_3N (2.0 mmol, 279.0 μL) solid $FeSO_4 \times 7H_2O$ (1.0 mmol, 278 mg) was added. The colorless reaction mixture was stirred until the color changed to yellow due to the complete dissolution of the iron salt. The subsequent addition of water at constant stirring resulted in the formation of dark-green solid product which turned tile red/rusty brown within 10-15 minutes, indicating Fe(II) oxidation. The precipitate was filtered off, washed with water, and dried in a desiccator (yield: 675 mg, 82%).

Methods for characterization of complex 1

Infrared (IR) spectra in the range of 4000-400 cm^{-1} were registered in KBr pellets on a Nicolet 6700 FT-IR spectrometer. Thermogravimetric experiments (TG-DTA/MS) were acquired with a Setaram Lab-sys Evo 1600 (25–600 °C, heating rate of 10 K/min in argon flow). The apparatus is equipped with an Omnistar GSD 301 O2 mass spectrometer. The electron paramagnetic resonance (EPR) studies were performed on a Bruker BioSpin EMXplus10/12 EPR spectrometer working at 9.4 GHz. ^{57}Fe Mössbauer measurements were carried out on a Wissel spectrometer operating in a constant acceleration mode. The transmission Mössbauer spectra were measured at room temperature (295 K) [25, 34]. The antibacterial tests were conducted in accordance with the experimental setup described previously, by determining the minimum inhibitory concentration (MIC) of the compounds of interest [36].

RESULTS AND DISCUSSION

Reaction of salinomycinic acid (SalH) with $FeSO_4 \times 7H_2O$ in the presence of Et_3N leads to the isolation of the Fe(III) complex (**1**) containing oxo, salinomycinate and hydroxo anions as ligands. We were not able to stabilize the low oxidation state of iron ions in oxygen environment and the physico-chemical characteristics of **1** suggest that it can be described as an isomer of $[Fe_3(\mu_3\text{-}O)Sal_3(OH)_4]$, a trinuclear Fe(III) salinomycinate **2**, already reported [25]. The amorphous nature of both species does not allow the use of the unambiguous single crystal X-ray diffraction, but certain differences in the spectral and magnetic behavior between the two compounds point to a possible rearrangement of their first coordination sphere.

The first evidence for the formation of complex **1** is given by IR spectroscopy (Fig. 2). Attention is drawn to particular regions, where the absorbance of several bonds provides useful information about the functional groups involved in interactions with iron ions. The intense peak at 1710 cm^{-1} in the spectrum of SalH (after applying a deconvolution procedure) is assigned to $\nu_{C=O}$ of carbonyl (1716 cm^{-1}) and carboxylic (1704 cm^{-1}) groups of the ligand. The carbonyl group of the antibiotic is not bound to the metal centre(s) in complexes **1** and **2**, demonstrated by the signals preserving their positions at 1716 cm^{-1}. These bands are of lower intensity compared to SalH at the expense of two new signals found at *ca.* 1528 cm^{-1} and 1419 cm^{-1}. They are assigned to asymmetric and symmetric vibrational modes of carboxylate group, respectively, which clearly indicate the deprotonation of salinomycin in **1** and **2** [25]. The deconvolution procedure applied to the composite signal belonging to the asymmetric COO^--stretch reveals that in the case of complex **1** it can be decomposed into three subbands at 1561, 1537 and 1524 cm^{-1}. The same band in **2** can be fitted only by two signals at 1533 and 1519 cm^{-1}. The observed differences in the positions of the asymmetric vibration of carboxylate function combined with some variations in Δ-values ($\Delta = \nu_{C=O}^{asym} - \nu_{C=O}^{sym}$) illustrate its bridging (although inequivalent) binding to the iron ions in the species **1** and **2** [37−40].

In the spectrum of SalH the intense asymmetric band at 3500 cm^{-1} with a shoulder at 3420 cm^{-1} is referred to ν_{OH} of hydroxyl groups some of which are engaged in hydrogen bonds formation.
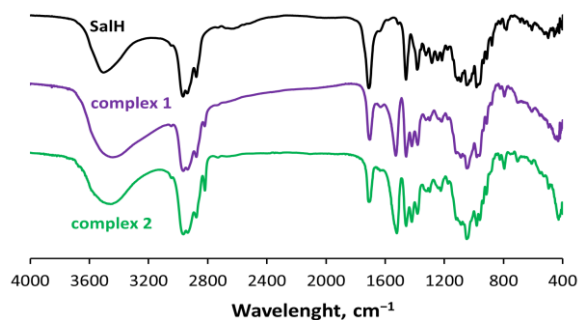
Fig. 2. IR spectra of SalH and complexes **1-2** (KBr pellets)

The OH-stretching vibrations appear in the spectra of **1** and **2** as much broader signals centred at 3447 cm^{-1} (**1**) and 3460 cm^{-1} (**2**), suggesting the participation of OH-group(s) of the antibiotic in interaction(s) with the heavy iron ion(s) in addition to H-bonds. In line with the reported ferric oxo-complex of salinomycin **2** [25], the thermal studies of species **1** (TG-DTA and TG-MS) exclude the presence of coordinated water molecules in the composition of the bulky sample.

The fingerprint region in the IR spectra of complexes **1** and **2** contains a signal at 1047 cm^{-1} not detectable in the spectrum of SalH. This band is assigned to the FeOH bending mode and serves as a proof for the presence of hydroxo group(s) directly bound to the metal centre in the structure of both coordination species. Another signal in the spectra of **1** and **2** which is not characteristic of SalH is detected at 430 cm^{-1} and relates to the stretch of Fe-O bond [41]. No evidence for the inclusion of sulfate anions into the composition of **1** is observed.

The IR and thermal analysis data reveal that complex **1** contains salinomycinate monoanion resulting from the deprotonation of its carboxylic group. The carboxylate function acts in a monodentate manner for binding to metal centre(s), but also serves as a bridge between two adjacent iron ions. Probably, the terminal OH-group of the antibiotic is involved in the primary coordination shell of metal ions, as well as hydroxo ligands originating from the basic conditions applied in the synthetic procedure of **1**.

The studies of magnetic properties undoubtedly demonstrated the inclusion of oxidized iron ions in the composition of complex **1**. The EPR spectra (Fig. 3), recorded in the range from 77 to 295 K, contain a single, relatively broad symmetric signal with Lorentz shape. The spectra broaden as the temperature decreases and the g-values increase from 2.02 to 2.15. The detection of broad EPR signals rise from the presence of individual Fe(III) ions ($^6S_{5/2}$) [25, 34, 42], which are exchange-coupled

in the structure of **1**. The temperature dependence of the linewidth could be explained by increased magnetic interactions at low temperatures. In many ferric monocarboxylate complexes these interactions occur through an oxo-anion centred in the core of the coordination compounds. The observed change in the g-factor contrasts to that detected for complex **2** [25] and can be explained by the existence of different types of Fe(III) nuclei. The EPR characteristics of our complex **1** corroborate the model of a trinuclear antiferromagnetically coupled cluster of Fe(III) ions. Combining EPR, IR and thermal data, we suggest that species **1** can be described as ferric oxo-complex encompassing salinomycinate and hydroxo ligands.
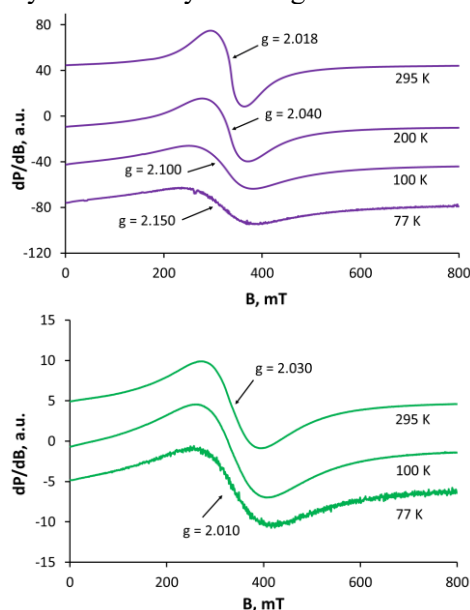

Fig. 3. X-band EPR temperature-dependent spectra of complexes **1** (top) and **2** (bottom [25])

The Mössbauer experiments in the absence of external magnetic field also confirm the oxidation state of iron ions in complex **1**. Its spectra at 293 K (Fig. 4) are fitted by two Lorentzian-shaped quadrupole-splitted doublets with relative intensity 2:1. The obtained subsites S1 and S2 are assigned to two different types of coordinated iron ions. The isomer shifts (IS) yielded by the least-square fitting (Table 1) are typical of high-spin iron(III) [43, 44]. The equivalence in IS values assumes that the strength of bond lengths at all irons is of the same order. The values of quadrupole splitting (QS), which describe the experimental signals of **1**, imply that two of the metal ions possess more symmetric charge distribution (0.59 mm/s) than the third one (0.96 mm/s) [45]. Thus, two of the ferric ions in **1** are indistinguishable by Mössbauer spectroscopy but the other one differs most likely due to the non-identical environment in its first coordination shell.
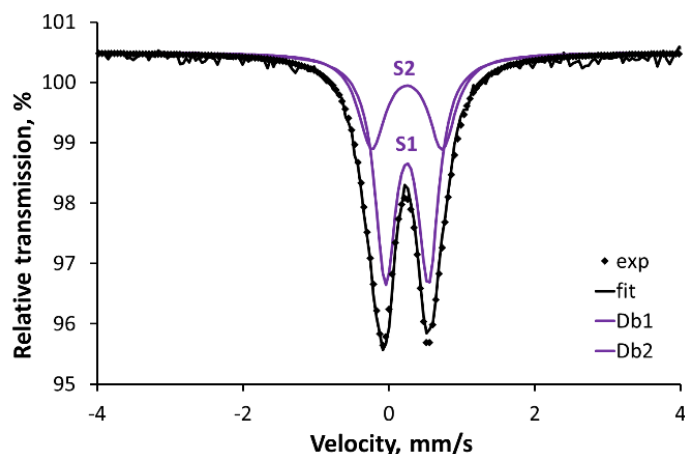
Fig. 4. Mössbauer spectrum of **1** at 295 K

Table 1. Mössbauer parameters of complexes **1** and **2**

Complex	Component	IS, mm/s	QS, mm/s	Γ*, mm/s	A**, %	Reference
1	Db1	0.36	0.59	0.35	64	This work
	Db2	0.36	0.96	0.45	36	
2	Db1	0.39	0.63	0.28	70	[25]
	Db2	0.38	0.80	0.49	30	

* **Γ** – signal linewidth; ** **A** – signal area

Table 2. MIC of SalH and complex **1**

Compound	MW	*B. cereus*		*B. subtilis*		*K. rhizophila*	
		μg/mL	μM	μg/mL	μM	μg/mL	μM
SalH	751.0	7.81	10.40	31.25	41.61	31.25	41.61
Complex **1**	2501.6	7.81	4.16	62.50	24.98	31.25	12.49

The observed Mössbauer peculiarities of complex **1** point to the formation of trinuclear ferric coordination species where the main donors are oxygen atoms. They derive from salinomycinate ligands in addition to oxo- and hydroxo-anions. The IS and QS values of complex **1** are similar but not identical with those of species **2** (Table 1), suggesting that irons in **1** are differently enveloped compared to complex **2**.

Without single crystal X-ray diffraction studies, we refrain to deduce the plausible structure of **1** but assume that it spans the $[Fe_3(\mu_3\text{-}O)Sal_3]^{4+}$ unit. We also imply that the positive charge of the discussed trinuclear ferric oxo-species is compensated by four hydroxo ions directly bound to the metal centres. The experimental data collected so far give rise to the hypothesis that the presented complex **1** can be treated as a new polymorph form of species **2** of total composition $[Fe_3(\mu_3\text{-}O)Sal_3(OH)_4]$. The question of the exact coordination mode of salinomycinate and hydroxo ligands in **1** remains open, and we hope to shed light on it in near future.

The preliminary studies on the antibacterial activity of SalH and **1** reveal that the strain of *B. cereus* is more susceptible to the effect of salinomycinic acid and its Fe(III) complex than *B. subtilis* and *K. rhizophila* (Table 2). The MIC values (μg/mL) of the studied samples are close to each other, but their activity can only be correctly interpreted when the exact composition of complex **1** becomes known. Considering the involvement of three salinomycinate and four hydroxo ligands into the structure of the triangular oxo-species **1**, we allude that the observed enhanced activity (μM) of **1** can be explained by the presence of biologically active antibiotic anions and the binding of Fe(III) ions preserves the antimicrobial effect of SalH towards the tested microorganisms.

CONCLUSION

Using ferrous ions, we isolated a ferric oxo-complex of the natural antibiotic salinomycin. The experimental data infer the coordination of the ionophore monoanions as bridging ligands, while the oxo-anion is responsible for the formation of a triangular antiferromagnetically coupled iron cluster. Magnetic studies definitely approve the oxidation of Fe(II) by the atmospheric oxygen

during the complex preparation and the presence of three metal centres which are inequivalent in a ratio of 2:1. The iron(III) ions retain the antimicrobial effect of salinomycin with the strain of *B. cereus* being more sensitive compared to *B. subtilis* and *K. rhizophila*.

REFERENCES

1. K. Y. Kim, S. H. Kim, S. N. Yu, S. G. Park, Y. W. Kim, H. W. Nam, H. H. An, H. S. Yu, Y. W. Kim, J. H. Ji, Y. K. Seo, S. C. Ahn, *Biomed. Pharmacother.*, **88**, 1016 (2017).
2. T. Kolenda, W. Przybyła, M. Kapałczyńska, A. Teresiak, M. Zajączkowska, R. Bliźniak, K. M. Lamperska, *Rep. Pract. Oncol. Radiother.*, **23**, 143 (2018).
3. J. Klose, S. Trefz, T. Wagner, L. Steffen, A. P. Charrier, P. Radhakrishnan, C. Volz, T. Schmidt, A. Ulrich, S. M. Dieter, C. Ball, H. Glimm, M. Schneider, *PLoS One,* **14**, e0211916 (2019).
4. M. Pérez-Hernández, A. Arias, D. Martínez-García, R. Pérez-Tomás, R. Quesada, V. Soto-Cerrato, *Cancers,* **11**, 1599 (2019).
5. M. Sulik, E. Maj, J. Wietrzyk, A. Huczyński, M. Antoszczak, *Biomolecules,* **10**, 1039 (2020).
6. S. Yao, W. Wang, B. Zhou, X. Cui, H. Yang, S. Zhang, *Exp. Ther. Med.,* **22**, 1390 (2021).
7. Y. Gao, Q. Shang, W. Li, W. Guo, A. Stojadinovic, C. Mannion, Y. G. Man, T. Chen, *J. Cancer,* **11**, 5135 (2020).
8. S. S. Kocoglu, C. Oy, M. Secme, F. B. Sunay, *Clin. Trans. Sci.,* **16**, 1725 (2023).
9. Y. Zhou, Y. Deng, J. Wang, Z. Yan, Q. Wei, J. Ye, J. Zhang, T.-C. He, M. Qiao, *Ann. Med.,* **55**, 954 (2023).
10. L. R. Chappel, *J. Parasitol.,* **65**, 137 (1979).
11. H. Mehlhorn, H. Pooch, W. Raether, *Z. Parasitenkd.,* **69**, 457 (1983).
12. M. Stallbaumer, K. J. Daisy, *Avian Pathol.*, **17**, 793 (1988).
13. S. Zhou, F. Wang, E. T. Wong, E. Fonkem, T. C. Hsieh, J. M. Wu, E. Wu, *Curr. Med. Chem.,* **20**, 4095 (2013).
14. C. Tan, H. Tan, J. Zhang, *Acta Microbiol. Sin.,* **56**, 1371 (2016).
15. A. Versini, L. Saier, F. Sindikubwabo, S. Müller, T. Cañeque, R. Rodriguez, *Tetrahedron,* **74**, 5585 (2018).
16. C. Naujokat, D. Fuchs, G. Opelz, *Mol. Med. Rep.,* **3**, 555 (2010).
17. C. Naujokat, R. Steinhart, *J. Biomed. Biotechnol.,* **2012**, 950658 (2012).
18. A. K. Sommer, A. Hermawan, F. M. Mickler, B. Ljepoja, P. Knyazev, C. Bräuchle, A. Ullrich, E. Wagner, A. Roidl, *Oncotarget,* **7**, 50461 (2016).
19. M. Norouzi, V. Yathindranath, J. A. Thliveris, D. W. Miller, *Nanomaterials (Basel),* **10**, 477 (2020).
20. M. Kusaczuk, E. T. Ambel, M. Naumowicz, G. Velasco, *Biochim. Biophys. Acta Rev. Cancer,* **1879**, 189054 (2024).
21. J. Ivanova, I. N. Pantcheva, R. Zhorova, G. Momekov, S. Simova, R. Stoyanova, E. Zhecheva, S. Ivanova, M. Mitewa, *J. Chem. Chem. Eng. David Publ.,* **6**, 551 (2012).
22. D. Momekova, G. Momekov, J. Ivanova, I. Pantcheva, E. Drakalska, N. Stoyanov, M. Guenova, A. Michova, K. Balashev, S. Arpadjan, M. Mitewa, S. Rangelov, N. Lambov, *J. Drug Deliv. Sci. Techn.,* **23**, 215 (2013).
23. V. N. Atanasov, S. S. Stoykova, Y. A. Goranova, A. N. Nedzhib, L. P. Tancheva, Ju. M. Ivanova, I. N. Pantcheva, *Bulg. Chem. Comm.,* **46**, 236 (2014).
24. I. Pantcheva, N. Petkov, S. Simova, R. Zhorova, P. Dorkov, *Phys. Sci. Rev.,* **8**, 3799 (2023).
25. N. Petkov, A. Tadjer, E. Encheva, Z. Cherkezova-Zheleva, D. Paneva, R. Stoyanova, R. Kukeva, P. Dorkov, I. Pantcheva, *Molecules,* **29**, 364 (2024).
26. Z. Li, L. Chen, C. Chen, Y. Zhou, D. Hu, J. Yang, Y. Chen, W. Zhuo, M. Mao, X. Zhang, L. Xu, L. Wang, J. Zhou, *Biomark. Res.,* **8**, 58 (2020).
27. Y. Su, B. Zhao, L. Zhou, Z. Zhang, Y. Shen, H. Lv, L. H. H. Al Qudsy, P. Shang, *Cancer Lett.,* **483**, 1247 (2020).
28. F. Chen, R. Kang, D. Tang, J. Liu, *J. Hematol. Oncol.,* **17**, 41(2024).
29. C. Fan, H. Wu, X. Du, C. Li, W. Zeng, L. Qu, C. Cang, *Cell Death Discov.,* **10**, 256 (2024).
30. R. Yu, Y. Hang, H. I. Tsai, D. Wang, H. Zhu, *Cancer Cell Int.,* **24**, 157 (2024).
31. T. Daimon, A. Bhattacharya, K. Wang, N. Haratake, A. Nakashoji, H. Ozawa, Y. Morimoto, N. Yamashita, T. Kosaka, M. Oya, D. W. Kufe, *Cell Death Discov.,* **10**, 9 (2024).
32. J. Feng, Z. X. Wang, J. L. Bin, Y. X. Chen, J. Ma, J. H. Deng, X. W. Huang, J. Zhou, G. D. Lu, *Cancer Lett.,* **587**, 216728 (2024).
33. Y. Y. Zhang, Y. Han, W. N. Li, R. H. Xu, H. Q. Ju, *Trends Pharmacol. Sci.,* **45**, 145 (2024).
34. N. Petkov, A. Tadjer, S. Simova, Z. Cherkezova-Zheleva, D. Paneva, R. Stoyanova, R. Kukeva, P. Dorkov, I. Pantcheva, *Inorganics,* **12**, 114 (2024)
35. P. G. Gertenbach, A. I. Popov, *J. Am. Chem. Soc.,* **97**, 4738 (1975).
36. N. Petkov, I. Pantcheva, A. Ivanova, R. Stoyanova, R. Kukeva, R. Alexandrova, A. Abudalleh, P. Dorkov, *Molecules,* **28**, 4676 (2023).
37. E. F. Paulus, M. Kurz, H. Matter, L. Vértesy, *J. Am. Chem. Soc.,* **120**, 8209 (1998).
38. V. Amani, N. Safari, H. R. Khavasi, *Spectrochim. Acta A: Mol. Biomol. Spectrosc.,* **85**, 17 (2012).
39. S. Kiana, M. Yazdanbakhsh, M. Jamialahmadi, S. F. Tayyari, *Spectrochim. Acta A: Mol. Biomol. Spectrosc.,* **130**, 287 (2014).

40. F. Dimiza, A. G. Hatzidimitriou, Y. Sanakis, A. N. Papadopoulos, G. Psomas, *J. Inorg. Biochem.,* **218**, 111410 (2021).
41. Q. Feng, B. Li, R. Du, F. Jiang, T. Liu, *Trans. Met. Chem.,* **44**, 49 (2019).
42. R. P. Chakradhar, G. Sivaramaiah, J. L. Rao, N. O. Gopal, *Spectrochim. Acta A: Mol. Biomol. Spectrosc.,* **62**, 51 (2005).
43. N. N. Greenwood, T. C. Gibb, Mössbauer Spectroscopy, Springer Dordrecht, 1971.
44. S. Murray, *Coord. Chem. Rev.,* **12**, 1 (1974).
45. E. Bill, C. Krebs, M. Winter, M. Gerdan, A. X. Trautwein, U. Florke, H.-J. Haupt, P. Chaudhuri, *Chem. Eur. J.,* **3**, 193 (1997).